Published in final edited form as:
J Immunol. 2007 July 1; 179(1): 382–390.

IL-4-STAT6 Signal Transduction-Dependent Induction of the Clinical Phase of Sjögren's Syndrome-Like Disease of the Nonobese Diabetic Mouse[1]

Cuong Q. Nguyen[2,*], **Jue-hua Gao**[3,†], **Hyuna Kim**[*], **Daniel R. Saban**[4,*], **Janet G. Cornelius**[†], and **Ammon B. Peck**[*,†,‡]

[*]Department of Oral Biology, College of Dentistry, University of Florida, Gainesville, FL 32610

[†]Department of Pathology, Immunology and Laboratory Medicine, College of Medicine, University of Florida, Gainesville, FL 32610

[‡]Center for Orphan Autoimmune Diseases, College of Dentistry, University of Florida, Gainesville, FL 32610

Abstract

NOD.B10-*H2*^{b} and NOD/LtJ mice manifest, respectively, many features of primary and secondary Sjögren's syndrome (SjS), an autoimmune disease affecting primarily the salivary and lacrimal glands leading to xerostomia (dry mouth) and xerophthalmia (dry eyes). B lymphocytes play a central role in the onset of SjS with clinical manifestations dependent on the appearance of autoantibodies reactive to multiple components of acinar cells. Previous studies with NOD.*IL4*$^{-/-}$ and NOD.B10-*H2*^{b}.*IL4*$^{-/-}$ mice suggest that the Th2 cytokine, IL-4, plays a vital role in the development and onset of SjS-like disease in the NOD mouse model. To investigate the molecular mechanisms by which IL-4 controls SjS development, a *Stat6* gene knockout mouse, NOD.B10-*H2*^{b}.C-*Stat6*$^{-/-}$, was constructed and its disease profile was defined and compared with that of NOD.B10-*H2*^{b}.C-*Stat6*$^{+/+}$ mice. As the NOD.B10-*H2*^{b}.C-*Stat6*$^{-/-}$ mice aged from 4 to 24 wk, they exhibited leukocyte infiltration of the exocrine glands, produced anti-nuclear autoantibodies, and showed loss and gain of saliva-associated proteolytic enzymes, similar to NOD.B10-*H2*^{b}.C-*Stat6*$^{+/+}$ mice. In contrast, NOD.B10-*H2*^{b}.C-*Stat6*$^{-/-}$ mice failed to develop glandular dysfunction, maintaining normal saliva flow rates. NOD.B10-*H2*^{b}.C-*Stat6*$^{-/-}$ mice were found to lack IgG1 isotype-specific anti-muscarinic acetylcholine type-3 receptor autoantibodies. Furthermore, the IgG fractions from NOD.B10-*H2*^{b}.C-*Stat6*$^{-/-}$ sera were unable to induce glandular dysfunction when injected into naive recipient C57BL/6 mice. NOD.B10-*H2*^{b}.C-*Stat6*$^{-/-}$ mice, like NOD.B10-*H2*^{b}. *IL4*$^{-/-}$ mice, are unable to synthesize IgG1 Abs, an observation that correlates with an inability to develop end-stage clinical SjS-like disease. These data imply a requirement for the IL-4/STAT6-pathway for onset of the clinical phase of SjS-like disease in the NOD mouse model.

[1]This work was supported in part by Public Health Service Grants DE013769, DE014344, and DE015152 (to A.B.P.) from the National Institutes of Health. C.Q.N. was supported by a postdoctoral fellowship from Public Health Service Grant T32 DE07200.

[2]Address correspondence and reprint requests to Dr. Cuong Q. Nguyen, Department of Oral Biology, College of Dentistry, University of Florida, P.O. Box 100424, Gainesville, FL 32610. nguyen@pathology.ufl.edu.
[3]Current address: Department of Pathology, Feinberg School of Medicine, Northwestern University, Chicago, IL 60611.
[4]Current address: Schepens Eye Research Institute, Harvard University, Boston, MA 02114.

Disclosures
The authors have no financial conflict of interest.

Sjögren's syndrome (SjS)[5] is a human autoimmune disease characterized by loss of exocrine function as a result of a chronic immune attack directed primarily against the salivary and lacrimal glands leading to xerostomia (dry mouth) and xerophthalmia (dry eyes) (1–4). Recent studies suggest that B cells and autoantibodies play an important role in the exocrine glandular dysfunction (5). Hyperproliferation and hyperactivity of autoreactive B lymphocytes result in severe hypergammaglobulinemia that is often found in patients with SjS and NOD mice (6,7). In addition, SjS patients, as well as NOD mice and some of its congenic partners, develop specific autoantibodies against nuclear Ags, intracellular components, membrane proteins, and secreted products of exocrine tissues (8–12).

Between 40 and 70% of all SjS patients' sera contain autoantibodies that are reactive to SS-A/Ro and/or SS-B/La Ags. These two specific anti-nuclear autoantibodies (ANAs) are now used as diagnostic markers of SjS despite being disease nonspecific (4). However, more recent reports have focused considerable attention on anti-muscarinic acetylcholine type-3 receptor (M3R) autoantibodies, although this point has proven to be difficult to define. Preliminary studies suggest that anti-M3R autoantibodies may be present in 40–60% of sera from SjS patients and 70–100% of NOD mice (13,14) and may be an important effector of glandular dysfunction by blocking normal signal transduction pathways possibly leading to the internalization of the Ab-receptor complexes or desensitizing acinar cells to normal neural stimulations (15–17). This concept is supported, indirectly, by a study showing that the IgG fractions of sera obtained from SjS patients or NOD mice with active disease can suppress stimulated salivary flow rates when infused into healthy, normal mice (5).

The possibility that anti-M3R autoantibodies may be involved in development of xerostomia and xerophthalmia in SjS has led us to examine this issue in greater detail. Earlier studies using a number of congenic partner strains of NOD and NOD.B10-$H2^b$ with non-functional cytokine genes revealed that the *IL-4* gene knockout (KO) mice, NOD. $IL4^{-/-}$ and NOD.B10-$H2^b$. $IL4^{-/-}$, failed to develop salivary gland dysfunction despite severe leukocytic infiltration of the salivary glands, accompanied by detectable increases in the expression of proinflammatory cytokines (18). Interestingly, both *NOD*.$IL4^{-/-}$ and NOD.B10-$H2^b$. $IL4^{-/-}$ mice failed to produce M3R autoantibodies of the IgG1 isotype (19,20). IL-4 is a pleiotropic cytokine involved in cell proliferation, activation, and differentiation (21). Function of this Th2 cytokine is known to be involved in two different signal transduction pathways, the IL-4-insulin receptor substrate (IRS) pathway responsible for cellular proliferation and activation, and the IL-4-STAT6 pathway indirectly controlling isotype switching in mice from IgM to IgE and IgG1 by specifically stimulating germline ε and γ1 Ig gene transcription (22,23). Even though IL-4 acting through the IRS pathway might be critical in activation and proliferation that results in the survival and expansion of autoreactive T and/or B cells, our recent studies have pointed to the requirement for IgG1 isotypic autoantibodies against M3R in the secretory dysfunction in NOD mice (19,20). In support of this concept, adoptive transfer of T cells capable of synthesizing IL-4 into NOD.B10-$H2^b$.$IL4^{-/-}$ mice incapable of producing IgG1/IgE resulted in salivary and lacrimal gland dysfunction that correlated with the production of the IgG1-M3R autoantibody (19). In the present study, the biological role of the IL-4-STAT6 pathway has been examined using our newly constructed *Stat6* gene KO mouse, NOD.B10-$H2^b$.C-$Stat6^{-/-}$.

[5]Abbreviations used in this paper: SjS, Sjögren's syndrome; ANA, anti-nuclear autoantibody; M3R, muscarinic acetylcholine type-3 receptor; KO, knockout; IRS, insulin receptor substrate; PSP, parotid secretory protein; LES, lymphoepithelial sialadenitis.

Materials and Methods

Animals

BALB/cJ and NOD/LtJ mice were bred under specific pathogen-free conditions in the mouse facility of the Department of Pathology (University of Florida, Gainesville, FL). Breeder pairs of NOD.B10-*H2*^{b} and C.129S2-*Stat6*^{tm1Gru}/J mice were purchased from The Jackson Laboratory. NOD.B10-*H2*^{b}.C-*Stat6*$^{-/-}$ mice were generated by crossing NOD.B10-*H2*^{b}.C-*Stat6*$^{-/-}$ males with NOD.B10-*H2*^{b} female mice. The F1 heterozygotes were intercrossed to produce F_2 generations that were screened for the presence and/or absence of the disrupted *Stat6* gene by PCR, and the MHC *H-2*^{b} locus by microsatellite marker genotyping. PCR primers for *Stat6* were purchased from Invitrogen Life Technologies. Microsatellite marker primers (Dmit) were based on sequences published by The Jackson Laboratory. Mice homozygous for both a neomycin-disrupted *Stat6* gene and the *H-2IA*^{b} gene were backcrossed to NOD.B10-*H2*^{b} mice to obtain mice heterozygous for the neomycin-disrupted *Stat6* gene. Such mice were backcrossed through six BC generations, at which time BC6 generation mice were intercrossed to obtain *Stat6*$^{-/-}$ gene KO, *Stat6*$^{+/-}$ heterozygous, and *Stat6*$^{+/+}$ wild-type mice. For convenience, we have designated these mice as NOD.B10-*H2*^{b}.C-*Stat6*$^{-/-}$, NOD.B10-*H2*^{b}.C-*Stat6*$^{+/-}$, and NOD.B10-*H2*^{b}.C-*Stat6*$^{+/+}$, respectively. Female mice were used throughout these studies, with the exception of collecting serum from both female and male NOD.B10-*H2*^{b}.C-*Stat6*$^{-/-}$ and NOD.B10-*H2*^{b}.C-*Stat6*$^{+/+}$ mice for use in the IgG fusion studies. It should be noted that previous studies have indicated SjS-like disease is more severe in females than males of the parental NOD.B10-*H2*^{b} strain. Mice were maintained in the Pathology Department's Mouse Facility where they received water and food ad libitum. The studies described herein were approved by the University of Florida Institutional Animal Care and Use Committee.

Determination of serum Ig isotypes

Measurements of individual Ig isotypes in sera samples were made using the Beadlyte Mouse Ig Isotyping kit (catalog no. 48–300; Upstate Biotechnology). All procedures were performed as per the manufacturer's instructions. In brief, diluted Beadlyte Mouse MultiImmunoglobulin standard and samples were added to each well of a filter 96-well plate. Sonicated Beadlyte Mouse Ig bead solution was added to each well and incubated in the dark at room temperature for 15 min. Mixtures were washed twice with PBS plus 0.05% Tween 20 (PBST) and resuspended in 75 μl of PBST. Reporter solution containing PE mouse Ig κ and λ L chain reporters were added to each well. The mixtures were incubated 15 min at room temperature on a plate shaker. Liquid from the plate was removed and then resuspended in 125 μl of PBST. The samples were measured using the Luminex 100 instrument.

IL-4 stimulation of CD19-positive B lymphocytes

Spleens were freshly explanted from euthanized mice and gently minced through a steel sieve. Following a single wash with PBS, the RBC were lysed by a 7-min exposure to 0.84% NH_4Cl. The resulting cell suspensions were washed two times in PBS, counted, and resuspended at 2×10^8 cells/ml in PBS supplemented to 2% FBS. Splenic B cell populations were isolated using the EasySep Mouse CD19 Positive Selection kit (catalog no. 18754; StemCell Technologies) as per the manufacturer's protocol. In brief, splenocytes suspended in EasySep Positive Selection mixture were treated with anti-CD19 Ab, then mixed with magnetic nanoparticles. CD19-positive cells were captured with a magnet and the supernatant was poured off. The magnetically labeled cells were washed and captured two more times. The purity of the isolated B cell preparations averaged ~94% as determined by flow cytometry.

CD19-positive B cell populations (5×10^5 cells/ml) were cultured in RPMI 1640 (Mediatech) supplemented to 10% FBS (HyClone), 2 mM L-glutamine (Mediatech), 0.05 mM 2-ME (Sigma-Aldrich), and 50 μg/ml penicillin/streptomycin (Invitrogen Life Technologies). Cultures were stimulated for 48 h with 20 ng/ml recombinant mIL-4 (catalog no. 550067; BD Biosciences/BD Pharmingen), after which time the cells were collected, stained with recombinant-PE-conjugated rat anti-mouse CD23 (catalog no. 553139; BD Biosciences/BD Pharmingen) and recombinant-PE-conjugated mouse anti-mouse I-A^b (catalog no. 553552; BD Biosciences/BD Pharmingen) mAbs, and examined for fluorescence by flow cytometry (FACScan; BD Biosciences).

Proteolysis of parotid secretory protein (PSP)

Detection of PSP proteolysis was conducted by incubating whole saliva specimens with a synthesized oligopeptide corresponding to amino acids 20–34 of the published sequence for mouse PSP. This oligopeptide contains the proteolytic site (NLNL) for a serine kinase activated in salivary glands during the development and onset of SjS-like disease in the NOD mouse (our unpublished data). Eight microliters of saliva collected from individual mice were mixed with 42 μl of the PSP oligopeptide (2.5 mg/ml) and incubated at 42°C for 12 h. Following incubation, 50 μl of Tris-HCl buffer (50 mM (pH 8.0)) was added and the mixture was centrifuged through Microspin filter tubes at 14,000 rpm for 10 min. The filtrates were analyzed by HPLC (Dionex Systems) for proteolytic products. Control samples consisted of 50 μl of the PSP oligopeptide.

Measurement of saliva flow rates

To measure stimulated flow rates of saliva, individual mice were weighed and given an i.p. injection of 0.1 ml of a mixture containing isoproterenol (1 mg/ml) and pilocarpine (2 mg/ml) dissolved in PBS. Saliva was collected for 10 min from the oral cavity of individual mice using a micropipette starting 1 min after injection of the secretagogue. The volume of each saliva sample was measured. The saliva samples were then frozen at −80°C until analyzed.

Detection of ANA in sera

ANA in the sera of mice were detected using the ANA screening kit (Immuno Concepts). Sera were tested at 1/40, 1/100, 1/500, and 1/1000 dilutions. Data are presented from the 1/40 dilutions. HEp-2-fixed substrate slides were overlaid with the appropriate mouse serum. Slides were incubated for 30 min at room temperature in a humidified chamber. After three washes for 5 min with PBS, the substrate slides were covered with various isotypic secondary FITC-conjugated goat anti-mouse Abs, specifically anti-Ig, anti-IgG1, anti-IgG2a, anti-IgG2b, anti-IgG3, and anti-IgM (Serotec) diluted 1/50 for 30 min at room temperature. After three washes, nuclear fluorescence was detected by fluorescence microscopy at ×200 magnification.

Ig subclass-specific anti-M3R autoantibody detection by flow cytometry

Detection of anti-M3R Abs in sera of NOD.B10-*H2*^{b}.C-*Stat6*$^{+/+}$ and NOD.B10-*H2*^{b}.C-*Stat6*$^{-/-}$ mice was determined using immunofluorescence. Flp-In CHO cells were transfected with the mouse *M3R* gene and selected for the antibiotic resistance. Newly selected M3R transfected Flp-in CHO and nontransfected Flp-In CHO were plated on multiwell slides with 50% confluence. Sera diluted at 1/50 in PBS were incubated with the cells for 1 h in a humidified chamber at room temperature. After incubation, cells were washed with PBS for five times, 5 min each. Isotypic FITC-conjugated secondary Abs, IgG1, IgG2a, IgG2b, IgG3, IgM, and IgG (Serotec) diluted at 1/100 were added, and

incubated for 30 min at 25°C. Cells were washed five times for 5 min/wash, and then visualized using a Zeiss Axiovert 200 M microscope (Carl Zeiss MicroImaging).

Histology

Submandibular glands were surgically removed from each mouse at the time of euthanasia (20–28 wk of age) and placed in 10% phosphate-buffered formalin for 24 h. Fixed tissues were embedded in paraffin and sectioned to 5-μm thickness. Paraffin-embedded slides were deparaffinized by immersing in xylene, followed by dehydration in ethanol. The tissue sections were stained with H&E dye (Gainesville Service Tech). Stained sections were observed at ×100 magnification for glandular structure and leukocyte infiltration.

Immunofluorescent staining for B and T lymphocytes

Paraffin-embedded tissues of the submandibular glands were sectioned and mounted onto microscope slides. Slides were deparaffinized by immersing in xylene, then dehydrated in ethanol. Following a 5-min wash with PBS at 25°C, the sections were incubated 1 h with blocking solution containing normal rabbit serum diluted 1/50 in PBS. Each section was incubated with rat anti-mouse B220 (BD Biosciences/BD Pharmingen) diluted 1/10 and goat anti-mouse CD3 (Santa Cruz Biotechnology) diluted 1/50 for 1 h at 25°C. The slides were washed three times with PBS for 5 min/wash followed by a 1-h incubation with Texas Red-conjugated rabbit anti-rat IgG (Biomeda) diluted 1/25 and FITC-conjugated rabbit anti-goat IgG (Sigma-Aldrich) diluted 1/100 at 25°C. The slides were washed thoroughly with PBS, treated with Vectashield DAPI-mounting medium (Vector Laboratories), and overlaid with glass coverslips. Stained sections were visualized at ×200 magnification.

Purification of IgG fraction and infusion into mice

Sera were isolated from whole blood collected from NOD.B10-*H2*^{b}.C-*Stat6*$^{+/+}$ and NOD.B10-*H2*^{b} .C-*Stat6*$^{-/-}$ mice aged 6 or 16 wk. Isolation of the IgG fractions from each serum sample was conducted using the Melon Gel IgG Purification kit (catalog no. 45212; Pierce), according to the manufacturer's instructions. The purities of the IgG fractions were determined by Coomassie blue staining and Western blot analyses on SDS/PAGE. The individual purified IgG fractions (500 μg in 200 μl of PBS) were injected into the i.p. cavities of male C57BL/6 mice starting at 12 wk of age. The in vivo physiological effect of injected IgG fractions on salivary gland secretory function of recipient mice was assessed by monitoring the saliva flow rates on days 1, 2, 3, and 5 postinfusion and comparing with saliva flow rates taken 1 day before infusion (day −1).

Statistical analyses

Differences in the levels of Ig isotypes and stimulated salivary flow rates were analyzed with the Student Newman-Keuls test or two-tailed paired Student's *t* test using GraphPad InStat software. Values of $p < 0.05$ were considered significant.

Results

Phenotypic comparison of NOD.B10-*H2*^{b}.C-*Stat6*$^{+/+}$ and NOD.B10-*H2*^{b}.C-*Stat6*$^{-/-}$ mice

NOD.B10-*H2*^{b}.C-*Stat6*$^{+/+}$ and NOD.B10-*H2*^{b}.C-*Stat6*$^{-/-}$ mice used in this study were offspring from interbreeding siblings after the sixth backcross to parental NOD.B10-*H2*^{b} mice. Theoretically, these mice would be ~99% of the NOD genetic background. To ensure that the predicted phenotypes were present in the BC6 NOD.B10-*H2*^{b}.C-*Stat6*$^{-/-}$ mice, the levels of serum IgE and IgG1 were determined, as STAT6 is required for Cε and Cγ1 germline transcription via its up-regulation of activation-induced cytidine deaminase in response to IL-4R stimulation by its ligand, IL-4 (21). As presented in Table I, the serum

levels of IgE and IgG1 in the NOD.B10-*H2*^{b}.C-*Stat6*$^{-/-}$ mice, as determined using a Luminex-based Beadlyte Mouse Ig Isotype kit, were reduced nearly 90% in comparison to levels present in NOD.B10-*H2*^{b}.C-*Stat6*$^{+/+}$ mice, and clearly reduced in comparison to levels present in a control strain like C57BL/6. Levels of IgM and IgA were also reduced (~2-fold) in NOD.B10-*H2*^{b}.C-*Stat6*$^{-/-}$ mice compared with NOD.B10-*H2*^{b}.C-*Stat6*$^{+/+}$ and C57BL/6 mice, while little or no differences were seen in IgG2a/c, IgG2b, and IgG3 isotypes between *Stat6* wild-type and KO mice.

In addition to IgE and IgG1, CD23 and MHC class II proteins are cell surface molecules whose expressions are also regulated through the activation of the IL-4/STAT6 signaling pathway (24,25). To examine the effect of the dysfunctional *Stat6* gene in the expression of these two molecules on B lymphocytes, CD19-positive B cells isolated from the spleens of NOD.B10-*H2*^{b}.C-*Stat6*$^{+/+}$ and NOD.B10-*H2*^{b}.C-*Stat6*$^{-/-}$ mice were stimulated for 48 h with 20 ng/ml rIL-4, then analyzed for expression levels of CD23 and MHC class Ags by flow cytometry. As shown in Fig. 1, a significant reduction in the expression levels of both I-A^{b} and the CD23 molecule in *Stat6*$^{-/-}$ mice was seen following stimulation with rIL-4 in comparison to the *Stat6*$^{+/+}$ wild-type mice. Similar results were obtained following stimulation of the B cell populations with LPS (data not presented). Taken together, the results of these two distinct down-stream attributes indicate that the *Stat6*$^{-/-}$ mice are presenting with a phenotype consistent with a dysfunctional *Stat6*$^{-/-}$ gene.

Pathophysiological characteristics of SjS-like disease in NOD.B10-*H2*^{b}.C-*Stat6*$^{+/+}$ and NOD.B10-*H2*^{b}.C-*Stat6*$^{-/-}$ mice

Although the underlying cause of SjS remains elusive, a number of studies using the NOD mouse model and its congenic partner strains have led us to propose the concept that this autoimmune exocrinopathy can be delineated into three consecutive, yet continuous phases (26,27). In the first phase, a number of aberrant genetic, physiological, and biochemical activities associated with retarded salivary gland organogenesis and acinar cell apoptosis occur, while in the second phase, leukocytes infiltrate the exocrine glands with a concomitant increase in the expression of inflammatory cytokines and production of autoantibodies. In the third phase, or onset of SjS-like clinical disease, secretory dysfunction of the salivary and lacrimal glands occurs, most likely the result of production and activity of anti-M3R autoantibodies (13,28). An interruption within any one of these three phases can prevent development of clinical disease.

To identify the early development of SjS-like disease in NOD mice, we commonly test for the appearance in saliva (or submandibular gland tissue lysates) of an activated serine kinase capable of proteolysis of PSP. Thus, to confirm that the NOD.B10-*H2*^{b}.C-*Stat6*$^{+/+}$ and NOD.B10-*H2*^{b}.C-*Stat6*$^{-/-}$ mice exhibited this manifestation, saliva collected from each mouse was tested for its ability to cleave PSP at the NLNL amino acid sequence present in the N terminus. As presented in Fig. 2, saliva from both NOD.B10-*H2*^{b}.C-*Stat6*$^{+/+}$ and NOD.B10-*H2*^{b}.C-*Stat6*$^{-/-}$ mice exhibited the ability to cleave the PSP oligopeptide into its two fragments. Proteolytic cleavage of PSP can be detected in both NOD.B10-*H2*^{b}.C-*Stat6*$^{+/+}$ and NOD.B10-*H2*^{b}.C-*Stat6*$^{-/-}$ mice as early as 12 wk of age. Thus, STAT6, as would be predicted, does not have any significant impact on the preimmune pathophysiological changes normally exhibited during the early onset of the autoimmune process in parental NOD and NOD.B10-*H2*^{b} mice.

Leukocyte infiltration of the submandibular and lacrimal glands is a critical criterion for identification of the autoimmune phase of SjS in both human and animal models. Although the number of leukocyte foci present in the salivary and lacrimal glands often does not correlate directly with disease or its severity, SjS patients and NOD-derived mouse strains exhibiting SjS-like disease typically have leukocytic infiltrates in their salivary glands

whose histological appearance is termed lymphoepithelial sialadenitis (LES). To determine whether NOD.B10-*H2*^{b}.C-*Stat6*$^{+/+}$ and NOD.B10-*H2*^{b}.C-*Stat6*$^{-/-}$ mice develop LES, the submandibular glands from female mice euthanized at 4, 8, 12, 16, and 25–28 wk of age were freshly explanted, fixed in formalin, embedded in paraffin, sectioned, and stained. As presented in Fig. 3, histological examinations revealed that multiple foci of leukocytic infiltrates in submandibular glands were seen in all three genetic groups: NOD.B10-*H2*^{b}, NOD.B10-*H2*^{b}.C-*Stat6*$^{+/+}$, and NOD.B10-*H2*^{b}.C-*Stat6*$^{-/-}$ mice. However, LES can be first detected at ~12 wk of age in all three genetic groups of animals. Immunohistological staining revealed that both the lymphocytic infiltrates present in submandibular and lacrimal glands (lacrimal gland data not shown) were comprised of similar numbers and distributions of CD3^{+} T cells and B220^{+} B cells localized in well-defined foci. Lastly, the severity of the leukocytic infiltration increased over time.

With the appearance of T and B lymphocytes within the salivary glands, there is a subsequent production of an increasing number of detectable serum autoantibodies (29–32). The presence of ANA, in particular anti-SS-A/Ro and anti-SS-B/La in the sera of human patients, is considered a major parameter in the diagnosis of clinical SjS disease (4). To identify ANA in the sera of NOD.B10-*H2*^{b}.C-*Stat6*$^{+/+}$ and NOD.B10-*H2*^{b}.C-*Stat6*$^{-/-}$ mice, individual animals were bled serially between 5 and 22 wk of age, the sera were collected and pooled according to age and gender, and tested on Hep-2 cells. The presence of ANA was visualized by staining with isotypic secondary FITC-conjugated goat anti-mouse Abs. Each serum was examined at 1/40, 1/100, 1/500, and 1/1000 dilutions. No positive staining was observed after the 1/100 dilutions. As presented in Fig. 4, both NOD.B10-*H2*^{b}.C-*Stat6*$^{+/+}$ and NOD.B10-*H2*^{b}.C-*Stat6*$^{-/-}$ mice exhibited similar patterns of ANA staining on Hep2 cells. Both *Stat6* wild-type and KO mice showed a homogeneous ANA staining pattern for polyvalent anti-Ig and anti-IgG2a, while displaying a mostly cytoplasmic staining pattern for anti-IgG3 and anti-IgM. The only noticeable difference was the fact that sera from NOD.B10-*H2*^{b}.C-*Stat6*$^{+/+}$ mice revealed slightly weaker IgG2b staining of Hep2 cells than NOD.B10-*H2*^{b}.C-*Stat6*$^{-/-}$ mice sera, possibly indicating lower IgG2b Ab titers against ANAs in *Stat6* wild-type animals despite having higher overall serum concentrations of IgG2b (see Table I). Interestingly, both NOD.B10-*H2*^{b}.C-*Stat6*$^{+/+}$ and NOD.B10-*H2*^{b}.C-*Stat6*$^{-/-}$ mice exhibited only low levels of IgG1 reactivity on Hep2 cells.

Onset of SjS-like disease concomitant with detection of IgG1 anti-M3R autoantibodies in NOD.B10-*H2*^{b}.C-*Stat6*$^{+/+}$ mice but not NOD.B10-*H2*^{b}.C-*Stat6*$^{-/-}$ mice

In the final phase, SjS-like disease is represented by the onset of glandular dysfunction characterized by the temporal loss of saliva and tear secretion concomitant with the appearance of leukocyte infiltrates within the exocrine glands. To measure changes in salivary flow rates of NOD.B10-*H2*^{b}.C-*Stat6*$^{+/+}$ and NOD.B10-*H2*^{b}.C-*Stat6*$^{-/-}$ mice, each animal was weighed and injected with a secretagogue containing isoproterenol and pilocarpine. Stimulated saliva secretions were collected and measured as described in *Materials and Methods*. As shown in Fig. 5, female NOD.B10-*H2*^{b}.C-*Stat6*$^{+/+}$ and NOD.B10-*H2*^{b}.C-*Stat6*$^{+/-}$ mice showed on average a 40% reduction in production of saliva between 4 and 24 wk of age. In contrast, in female NOD.B10-*H2*^{b}.C-*Stat6*$^{-/-}$ mice, while showing a slight reduction in flow rates over this same time frame, this reduction proved not to be statistically significant. Thus, NOD.B10-*H2*^{b}.C-*Stat6*$^{+/+}$ and NOD.B10-*H2*^{b}.C-*Stat6*$^{+/-}$ mice exhibit a natural onset of exocrine dysfunction, while the *Stat6* KO NOD.B10-*H2*^{b}.C-*Stat6*$^{-/-}$ mice appear to retain normal secretory function of the salivary glands.

The polyclonal and monoclonal proliferations of autoreactive B lymphocytes in SjS disease of humans and NOD mice are known to lead to production of high levels of organ-specific and organ-nonspecific autoantibodies that correspond to the progression of disease (7). Such Abs include anti-SS-A/Ro and anti-SS-B/La in SjS patients (but not in NOD mice) (11),

rheumatoid factor (29), anti-fodrin, anti-carbonic anhydrase-II, ANA, and anti-M3R (27). Recent studies have focused on anti-M3R autoantibodies as they may be involved as effectors of glandular dysfunction (5). Considering the fact that NOD.B10-*H2*^{b}.C-*Stat6*$^{+/+}$ and NOD.B10-*H2*^{b}.C-*Stat6*$^{+/-}$ mice lose exocrine gland secretory function while NOD.B10-*H2*^{b}.C-*Stat6*$^{-/-}$ littermates retain exocrine function, it was imperative to determine the presence or absence of isotypic anti-M3R Abs.

To identify the presence of anti-M3R autoantibodies, we used the recently described Flp-In CHO cells transfected to overexpress the mouse *M3R* gene (14). As shown in Fig. 6, sera from NOD.B10-*H2*^{b}.C-*Stat6*$^{-/-}$ mice failed to stain the M3R-transfected CHO cells when counterstained with an anti-IgG1 secondary Ab. In contrast, these same sera exhibited staining of the target cells when counterstained with anti-IgG, anti-IgM, and IgG2b secondary antisera. Sera collected from the NOD.B10-*H2*^{b}.C-*Stat6*$^{+/+}$ littermates proved positive for IgM, IgG, IgG1, and IgG2b anti-M3R autoantibodies. All three sets of mice were negative for IgG2a and IgG3 anti-M3R autoantibodies (data not shown). Thus, the one obvious difference between NOD.B10-*H2*^{b}.C-*Stat6*$^{+/+}$ and NOD.B10-*H2*^{b}.C-*Stat6*$^{-/-}$ mice appears to be the absence of IgG1-anti-M3R autoantibody in the *Stat6* KO animals, thereby mimicking results from NOD.B10-*H2*^{b}.*IL4*$^{-/-}$ mice (19).

Normal salivary gland secretory function in C57BL/6 mice treated with serum IgG from NOD.B10-*H2*^{b}.C-*Stat6*$^{-/-}$, but not from NOD.B10-*H2*^{b}.C-*Stat6*$^{+/+}$, mice

Both primary SjS patients and NOD mice produce autoantibodies that interact with the autonomic nervous system receptors responsible for initiating the secretory response. Data thus far presented have suggested that NOD.B10-*H2*^{b}.C-*Stat6*$^{-/-}$ mice do not develop a clinical SjS-like disease due to the lack of production of IgG1 anti-M3R autoantibodies reported to be the effectors of glandular dysfunction (19,20). If this concept is correct, then infusions of IgG from NOD.B10-*H2*^{b}.C-*Stat6*$^{-/-}$ mice should have little or no effect on salivary gland function, whereas infusions of IgG from NOD.B10-*H2*^{b}.C-*Stat6*$^{+/+}$ mice exhibiting SjS-like disease should induce a temporary disease phenotype (5). Therefore, an experiment was conducted in which purified IgG fractions isolated from individual NOD.B10-*H2*^{b}.C-*Stat6*$^{+/+}$ and NOD.B10-*H2*^{b}.C-*Stat6*$^{-/-}$ mice were injected into normal C57BL/6 mice. As indicated in Fig. *7A*, mice receiving an injection of IgG from 6-wk-old NOD.B10-*H2*^{b}.C-*Stat6*$^{+/+}$ mice showed a short-term increase in their saliva flow rates within 48 h. In contrast, mice that received an injection of IgG from 6-wk-old NOD.B10-*H2*^{b}.C-*Stat6*$^{-/-}$ mice exhibited no significant changes in saliva flow rates. However, as shown in Fig. *7B*, mice injected with purified IgG from 16-wk-old NOD.B10-*H2*^{b}.C-*Stat6*$^{+/+}$ mice, known to manifest SjS-like disease, resulted in an average of 40% decrease in saliva flow rates. C57BL/6 mice, in contrast, displayed no changes in saliva flow rates following injection of IgG from 16-wk-old NOD.B10-*H2*^{b}.C-*Stat6*$^{-/-}$ mice. Thus, these data indicate that a single injection of IgG from prediseased and diseased NOD.B10-*H2*^{b}.C-*Stat6*$^{+/+}$ can induce a short-term effect on the salivary gland, whereas IgG from NOD.B10-*H2*^{b}.C-*Stat6*$^{-/-}$ mice, regardless of age, could not.

Discussion

In the present studies, we investigated the importance of STAT6 in the IL-4 signal transduction pathway for the development of SjS-like disease in the NOD mouse using our recently constructed *Stat6-gene* KO mouse referred to as NOD.B10-*H2*^{b}.C-*Stat6*$^{-/-}$. The NOD.B10-*H2*^{b}.C-*Stat6*$^{-/-}$ mouse was generated to further examine the role of STAT6 in isotype switching in SjS-like autoimmune exocrinopathy. As presented, NOD.B10-*H2*^{b}.C-*Stat6*$^{-/-}$ mice exhibited a number of characteristics observed in disease-prone NOD/Lt and NOD.B10-*H2*^{b} mice (19,20). These included 1) the presence of leukocyte infiltrations of the submandibular and lacrimal glands (the latter data not shown), 2) the production of ANA

and autoantibodies reactive with tissues of the salivary glands, and 3) the activation of a PSP-specific serine kinase protease. Most importantly, NOD.B10-*H2*^{b}.C-*Stat6*$^{-/-}$ mice also behaved like NOD.B10-*H2*^{b}.*IL4*$^{-/-}$ mice in that they failed to produce IgG1-M3R-specific autoantibodies and failed to exhibit the temporal loss of stimulated salivary flow rates.

Earlier studies using the *NOD.IL4*$^{-/-}$ and NOD.B10-*H2*^{b}.*IL4*$^{-/-}$ mice indicated that secretory function of salivary glands was restored to normal levels when the *Il4* gene was genetically knocked out, despite exhibiting the pathophysiological abnormalities and leukocyte infiltrations in the exocrine glands concomitantly with production of ANAs (19,20). These earlier data suggested that IL-4 plays an important role during the clinical phase, while having little or no effect on the pathology associated with preclinical disease state (phase I or II) of the SjS-like disease. IL-4, therefore, signaling via either the STAT-6 or IRS pathway, appears capable of regulating physiological functions that subsequently modulate the secretory activities of exocrine glands. Interestingly, *Il4* gene KO mice fail to produce IgG1 isotypic autoantibodies against M3R, yet produce normal levels of M3R of other isotypes, e.g., IgG2a, IgG2b, IgG3, IgM, and IgA, pointing to a critical role in IgG1 isotype switching (19). As previously discussed, IL-4 mediates its function via two separate pathways: the IL-4-IRS pathway responsible for cellular proliferation, activation, and survival, and the IL-4-STAT6 pathway involved in isotype switching to IgG1 and IgE by specifically stimulating germline γ1 and ε Ig gene transcription. As shown in the current study, NOD.B10-*H2*^{b}.C-*Stat6*$^{-/-}$ mice failed to make IgG1 Ab against M3R and purified IgG fractions from these mice failed to induce a temporary effect on saliva flow rates when infused into naive C57BL/6 mice, suggesting a crucial role for IgG1 anti-M3R Abs in effecting secretory dysfunction.

Although a variety of possible mechanisms leading to secretory dysfunction in the salivary and lacrimal glands are under intensive investigation, recent attention has focused on the role of anti-muscarinic receptor autoantibodies. Several hypotheses have surfaced including 1) blocking the muscarinic receptors from binding the neurotransmitter, acetylcholine, thereby preventing signal transductions regulating secretion (15), 2) internalization of the muscarinic receptors following their binding with autoantibodies, thereby resulting in decreased expression of the receptors on the acinar cells (17), and 3) a constant stimulation of the muscarinic receptors by autoantibody binding that results in overstimulation, thereby leading to acinar cell desensitization and reduced capacity for secretion (33).

The observations that clinical signs of SjS-like disease in our animal models appear to be mediated solely by IgG1 isotype-specific Abs reactive against the muscarinic receptors raises questions as to the relevance of the NOD mouse model to human SjS. In SjS patients, numerous autoantibodies have been identified, the more important ones being Abs reactive with intracellular ribonuclear proteins, in particular Ro/SS-A and La/SS-B (27). Autoantibodies to these nuclear proteins can be of either IgM, IgG, or IgA (29), with titers of IgA isotype-specific autoantibodies to Ro/SS-A and La/SS-B Ags correlating with sicca syndrome in primary SjS (29). In addition, levels of anti-Ro/SS-A and anti-La/SS-B have been reported to show a strong association with the titers of rheumatoid factor prevalent in patients with primary SjS (11), and while the levels of rheumatoid factor were not directly related to the disease state, they were highly significant in those patients developing extraglandular manifestations (11). In contrast, both SjS patients and NOD mice can produce anti-fodrin, anti-carbonic anhydrase II, and anti-nuclear autoantigens, none of which appear to mediate clinical disease, but represent markers of the ongoing pathophysiological changes in the salivary and lacrimal glands during onset of SjS (27). Interestingly, a similar dichotomy may be present in systemic lupus erythematosus-prone mice where IgG2a and IgG3 autoantibodies are considered pathogenic, whereas the predominant autoantibodies and Igs deposited in the kidneys are IgG1 and/or IgE isotypes

(34,35). Furthermore, knocking out either the *Il4* or *Stat6* gene in systemic lupus erythematosus-prone mouse models (e.g., BXSB, (MRL$^{lpr/lpr}$× C57BL/6)F_2, and NZM. 2410) has little effect on the production of autoantibodies and the degree of lymphocytic infiltrations into the secondary lymphoid organs or kidneys (36,37), observations consistent with our findings in the NOD.B10-*H2*^{b}.C-*Stat6*$^{-/-}$ mice.

How IgG1 isotype-specific anti-M3R Abs mediate exocrine gland dysfunction, whereas other isotype-specific anti-M3R Abs do not, remains to be explained, especially in light of our previous observations indicating that Fab isolated from IgG fractions of sera collected from either SjS patients or diseased NOD mice are fully capable of either stimulating or suppressing salivary flow rates in a reversible manner when infused into NOD.*Igμ*$^{-/-}$ or NOD.B10-*H2*^{b}.*Igμ*$^{-/-}$ mice (5). On one hand, there may be variable regions uniquely expressed by IgG1 Abs, a few of which recognize epitopes that can interfere functionally with muscarinic receptors. Alternatively, one could also postulate that *Stat6* may be involved in signal transduction pathways regulating processes involved in autoimmunity other than that for IL-4-dependent IgG1 isotype switching. Thus, the precise association of *Stat6* with clinical onset of SjS-like disease will require further studies.

References

1. Fox RI, Kang HI. Pathogenesis of Sjögren's syndrome. Rheum. Dis. Clin. North Am 1992;18:517–538. [PubMed: 1323135]
2. Fox RI, Michelson P. Approaches to the treatment of Sjögren's syndrome. J. Rheumatol 2000;61:15–21.
3. Jonsson R, Haga HJ, Gordon TP. Current concepts on diagnosis, autoantibodies and therapy in Sjögren's syndrome. Scand. J. Rheumatol 2000;29:341–348. [PubMed: 11132201]
4. Vitali C, Bombardieri S, Jonsson R, Moutsopoulos HM, Alexander EL, Carsons SE, Daniels TE, Fox PC, Fox RI, Kassan SS, et al. Classification criteria for Sjögren's syndrome: a revised version of the European criteria proposed by the American-European Consensus Group. Ann. Rheum. Dis 2002;61:554–558. [PubMed: 12006334]
5. Robinson CP, Brayer J, Yamachika S, Esch TR, Peck AB, Stewart CA, Peen E, Jonsson R, Humphreys-Beher MG. Transfer of human serum IgG to non-obese diabetic Igμ null mice reveals a role for autoantibodies in the loss of secretory function of exocrine tissues in Sjögren's syndrome. Proc. Natl. Acad. Sci. USA 1998;95:7538–7543. [PubMed: 9636185]
6. Robinson CP, Yamachika S, Bounous DI, Brayer J, Jonsson R, Holmdahl R, Peck AB, Humphreys-Beher MG. A novel NOD-derived murine model of primary Sjögren's syndrome. Arthritis Rheum 1998;41:150–156. [PubMed: 9433880]
7. Sugai S, Masaki Y, Dong L. Lymphoproliferative disorders in patients with Sjögren's syndrome. Autoimmun. Rev 2004;3:S67–0. [PubMed: 15309805]
8. Kino-Ohsaki J, Nishimori I, Morita M, Okazaki K, Yamamoto Y, Onishi S, Hollingsworth MA. Serum antibodies to carbonic anhydrase I and II in patients with idiopathic chronic pancreatitis and Sjögren's syndrome. Gastroenterology 1996;110:1579–1586. [PubMed: 8613065]
9. Feist E, Kuckelkorn U, Dorner T, Donitz H, Scheffler S, Hiepe F, Kloetzel PM, Burmester GR. Autoantibodies in primary Sjögren's syndrome are directed against proteasomal subunits of the α and β type. Arthritis. Rheum 1999;42:697–702. [PubMed: 10211883]
10. Billaut-Mulot O, Cocude C, Kolesnitchenko V, Truong MJ, Chan EK, Hachula E, de la Tribonniere X, Capron A, Bahr GM. SS-56, A novel cellular target of autoantibody responses in Sjögren's syndrome and systemic lupus erythematosus. J. Clin. Invest 2001;108:861–869. [PubMed: 11560955]
11. Harley JB, Alexander EL, Bias WB, Fox OF, Provost TT, Reichlin M, Yamagata H, Arnett FC. Anti-Ro (SS-A) and anti-La (SS-B) in patients with Sjögren's syndrome. Arthritis Rheum 1986;29:196–206. [PubMed: 3485431]

12. Haneji N, Nakamura T, Takio K, Yanagi K, Higashiyama H, Saito I, Noji S, Sugino H, Hayashi Y. Identification of α-fodrin as a candidate autoantigen in primary Sjögren's syndrome. Science 1997;276:604–607. [PubMed: 9110981]
13. Nguyen KH, Brayer J, Cha S, Diggs S, Yasunari U, Hilal G, Peck AB, Humphreys-Beher MG. Evidence for anti-muscarinic acetylcholine receptor antibody-mediated secretory dysfunction in *nod* mice. Arthritis Rheum 2000;43:2297–2306. [PubMed: 11037890]
14. Gao J, Cha S, Jonsson R, Opalko J, Peck AB. Detection of anti-type 3 muscarinic acetylcholine receptor autoantibodies in the sera of Sjögren's syndrome patients by use of a transfected cell line assay. Arthritis Rheum 2004;50:2615–2621. [PubMed: 15334476]
15. Waterman SA, Gordon TP, Rischmueller M. Inhibitory effects of muscarinic receptor autoantibodies on parasympathetic neurotransmission in Sjögren's syndrome. Arthritis Rheum 2000;43:1647–1654. [PubMed: 10902771]
16. Cavill D, Waterman SA, Gordon TP. Antiidiotypic antibodies neutralize autoantibodies that inhibit cholinergic neurotransmission. Arthritis Rheum 2003;48:3597–3602. [PubMed: 14674012]
17. Li J, Ha YM, Ku NY, Choi SY, Lee SJ, Oh SB, Kim JS, Lee JH, Lee EB, Song YW, Park K. Inhibitory effects of autoantibodies on the muscarinic receptors in Sjögren's syndrome. Lab. Invest 2004;84:1430–1438. [PubMed: 15448705]
18. Robinson CP, Cornelius J, Bounous DE, Yamamoto H, Humphreys-Beher MG, Peck AB. Characterization of the changing lymphocyte populations and cytokine expression in the exocrine tissues of autoimmune NOD mice. Autoimmunity 1998;27:29–44. [PubMed: 9482205]
19. Gao J, Killedar S, Cornelius JG, Nguyen C, Cha S, Peck AB. Sjögren's syndrome in the NOD mouse model is an interleukin-4 time-dependent, antibody isotype-specific autoimmune disease. J. Autoimmun 2006;26:90–103. [PubMed: 16413168]
20. Brayer JB, Cha S, Nagashima H, Yasunari U, Lindberg A, Diggs S, Martinez J, Goa J, Humphreys-Beher MG, Peck AB. IL-4-dependent effector phase in autoimmune exocrinopathy as defined by the NOD.IL-4-gene knockout mouse model of Sjögren's syndrome. Scand. J. Immunol 2001;54:133–140. [PubMed: 11439159]
21. Nelms K, Keegan AD, Zamorano J, Ryan JJ, Paul WE. The IL-4 receptor: signaling mechanisms and biologic functions. Annu. Rev. Immunol 1999;17:701–738. [PubMed: 10358772]
22. Singh RR. IL-4 and many roads to lupus-like autoimmunity. Clin. Immunol. Immunopathol 2003;108:73–79.
23. Linehan LA, Warren WD, Thompson PA, Grusby MJ, Berton MT. STAT6 is required for IL-4-induced germline Ig gene transcription and switch recombination. J. Immunol 1998;161:302–310. [PubMed: 9647237]
24. Takeda K, Tanaka T, Shi W, Matsumoto M, Minami M, Kashiwamura S, Nakanishi K, Yoshida N, Kishimoto T, Akira S. Essential role of Stat6 in IL-4 signaling. Nature 1996;380:627–630. [PubMed: 8602263]
25. Shimoda K, van Deursen J, Sangster MY, Sarawar SR, Carson RT, Tripp RA, Chu C, Quelle FW, Nosaka T, Vignali DA, et al. Lack of IL-4-induced Th2 response and IgE class switching in mice with disrupted Stat6 gene. Nature 1996;380:630–633. [PubMed: 8602264]
26. Brayer JB, Humphreys-Beher MG, Peck AB. Sjögren's syndrome: immunological response underlying the disease. Arch. Immunol. Ther. Exp 2001;49:353–360.
27. Cha S, Peck AB, Humphreys-Beher MG. Progress in understanding autoimmune exocrinopathy using the non-obese diabetic mouse: an update. Crit. Rev. Oral Biol. Med 2002;13:5–16. [PubMed: 12097234]
28. Jonsson, R.; Dowman, SJ.; Gordon, T. Sjögren's Syndrome. In: Koopman, WJ.; Moreland, LW., editors. Arthritis and Allied Conditions—A Textbook in Rheumatology. 15th Ed.. Philadelphia: Lippincott Williams & Wilkins; 2004. p. 1681-1705.
29. Pourmand N, Wahren-Herlenius M, Gunnarsson I, Svenungsson E, Lofstrom B, Ioannou Y, Isenberg DA, Magnusson CG. Ro/SSA and La/SSB specific IgA autoantibodies in serum of patients with Sjögren's syndrome and systemic lupus erythematosus. Ann. Rheum. Dis 1999;58:623–629. [PubMed: 10491361]

30. Maran R, Dueymes M, Pennec YL, Casburn-Budd R, Shoenfeld Y, Youinou P. Predominance of IgG1 subclass of anti-Ro/SSA, but not anti-La/SSB antibodies in primary Sjögren's syndrome. J. Autoimmun 1993;6:379–387. [PubMed: 8397718]

31. Aparisi L, Farre A, Gomez-Cambronero L, Martinez J, De Las Heras G, Corts J, Navarro S, Mora J, Lopez-Hoyos M, Sabater L, et al. Antibodies to carbonic anhydrase and IgG4 levels in idiopathic chronic pancreatitis: relevance for diagnosis of autoimmune pancreatitis. Gut 2005;54:703–709. [PubMed: 15831920]

32. Harley JB, Alexander EL, Bias WB, Fox OF, Provost TT, Reichlin M, Yamagata H, Arnett FC. Anti-Ro (SS-A) and anti-La (SS-B) in patients with Sjögren's syndrome. Arthritis Rheum 1986;29:196–206. [PubMed: 3485431]

33. Cha S, Singson E, Cornelius J, Yagna JP, Knot HJ, Peck AB. Muscarinic acetylcholine type-3 receptor desensitization due to chronic exposure to Sjögren's syndrome-associated autoantibodies. J. Rheumatol 2006;33:296–306. [PubMed: 16465661]

34. Ohnishi K, Ebling FM, Mitchell B, Singh RR, Hahn BH, Tsao BP. Comparison of pathogenic and non-pathogenic murine antibodies to DNA: antigen binding and structural characteristics. Int. Immunol 1994;6:817–830. [PubMed: 8086372]

35. Takahashi S, Fossati L, Iwamoto M, Merino R, Motta R, Kobayakawa T, Izui S. Imbalance towards Th1 predominance is associated with acceleration of lupus-like autoimmune syndrome in MRL mice. J. Clin. Invest 1996;97:1597–1604. [PubMed: 8601623]

36. Kono DH, Balomenos D, Park MS, Theofilopoulos AN. Development of lupus in BXSB mice is independent of IL-4. J. Immunol 2000;164:38–42. [PubMed: 10604990]

37. Singh RR, Saxena V, Zang S, Li L, Finkelman FD, Witte DP, Jacob CO. Differential contribution of IL-4 and STAT6 vs. STAT4 to the development of lupus nephritis. J. Immunol 2003;170:4818–4825. [PubMed: 12707364]

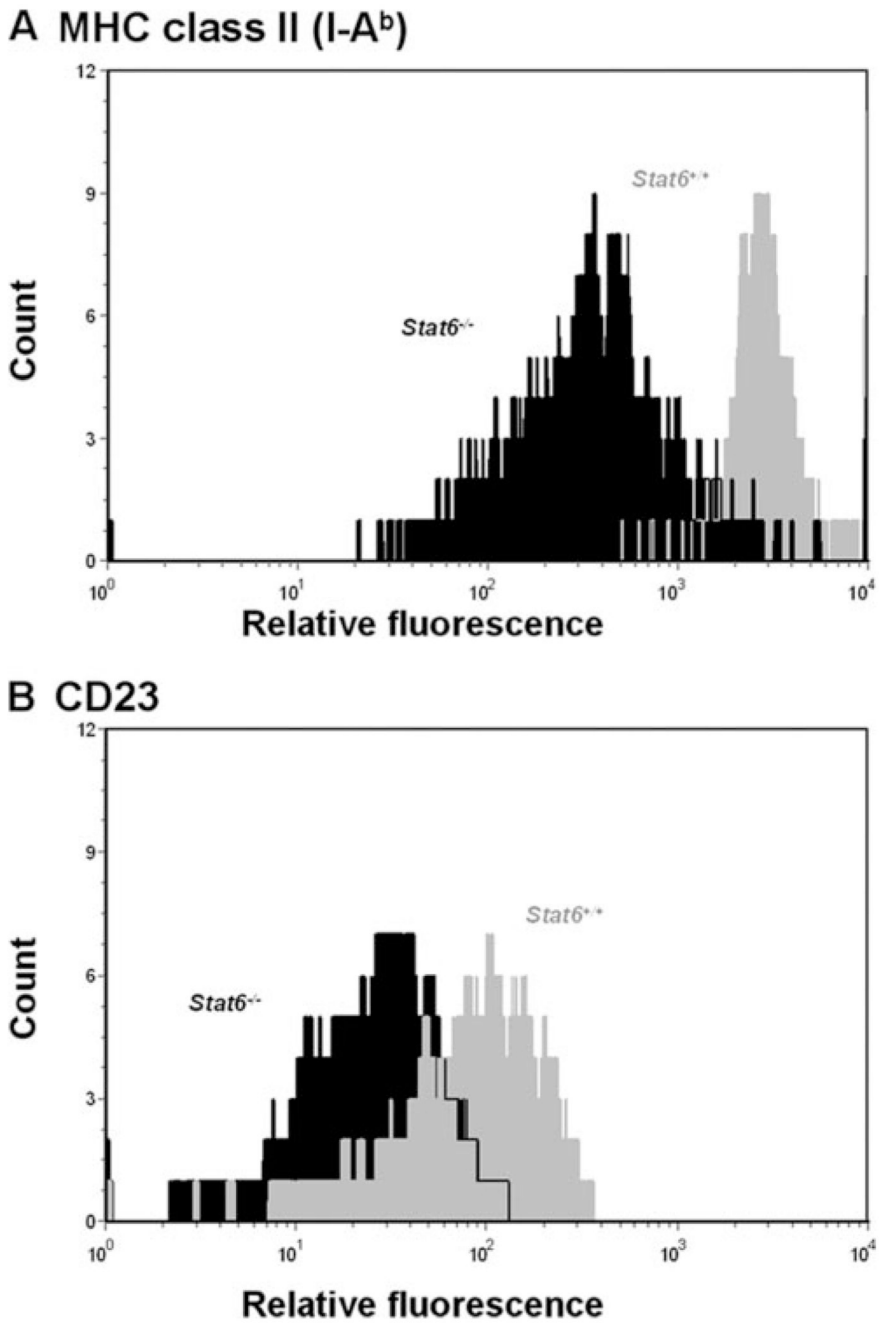

FIGURE 1.

Expression of MHC class II (I-A^b) and CD23 on B cells following IL-4 stimulation in vitro. Purified B lymphocytes from NOD.B10-*H2*^{b}.C-*Stat6*$^{+/+}$ and NOD.B10-*H2*^{b}.C-*Stat6*$^{-/-}$ mice were cultured in medium and stimulated for 48 h with 20 ng/ml recombinant mIL-4. After 48 h, cells were harvested and analyzed for MHC class II (I-A^b) and CD23 expression using flow cytometry. *A*, MHC class II (I-A^b) expression. *B*, CD23 expression. Gray, NOD.B10-*H2*^{b}.C-*Stat6*$^{+/+}$ mice. Black, NOD.B10-*H2*^{b}.C-*Stat6*$^{-/-}$ mice.

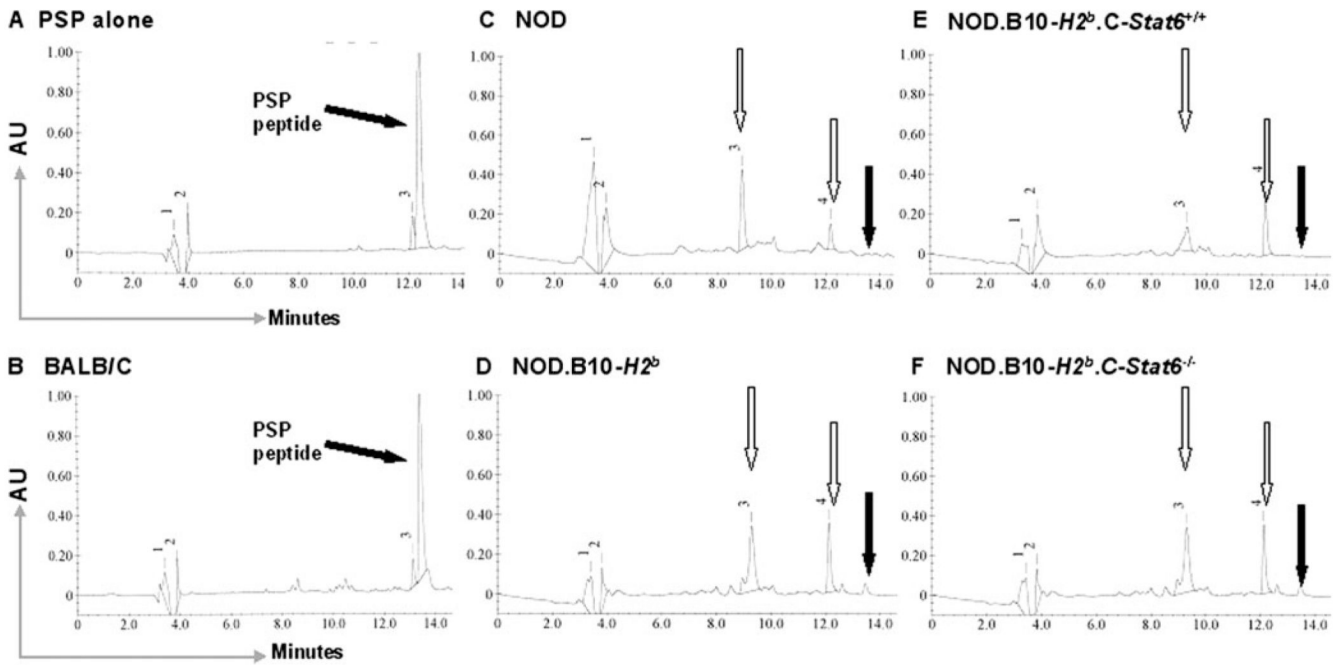

FIGURE 2.

Detection of proteolytic activity against PSP in saliva. Saliva, collected from individual mice, was assayed for proteolytic activity on a 16-mer oligopeptide containing the NLNL enzymatic site for a disease-activated serine kinase. Using reverse-phase HPLC, the synthetic 16-mer oligopeptide eludes at 13.9 min (*A*). Saliva from BALB/c mice was incapable of enzymatically digesting the oligopeptide (*B*). Saliva from NOD/LtJ (*C*), NOD.B10-*H2*^{b} (*D*), NOD.B10-*H2*^{b}.C-*Stat6*$^{+/+}$(*E*), and NOD.B10-*H2*^{b}.C-*Stat6*$^{-/-}$ (*F*) mice all showed full digestion of the oligopeptide with the two degradation products of the oligopeptide eluting at 9.2 and 12.8 min, respectively.

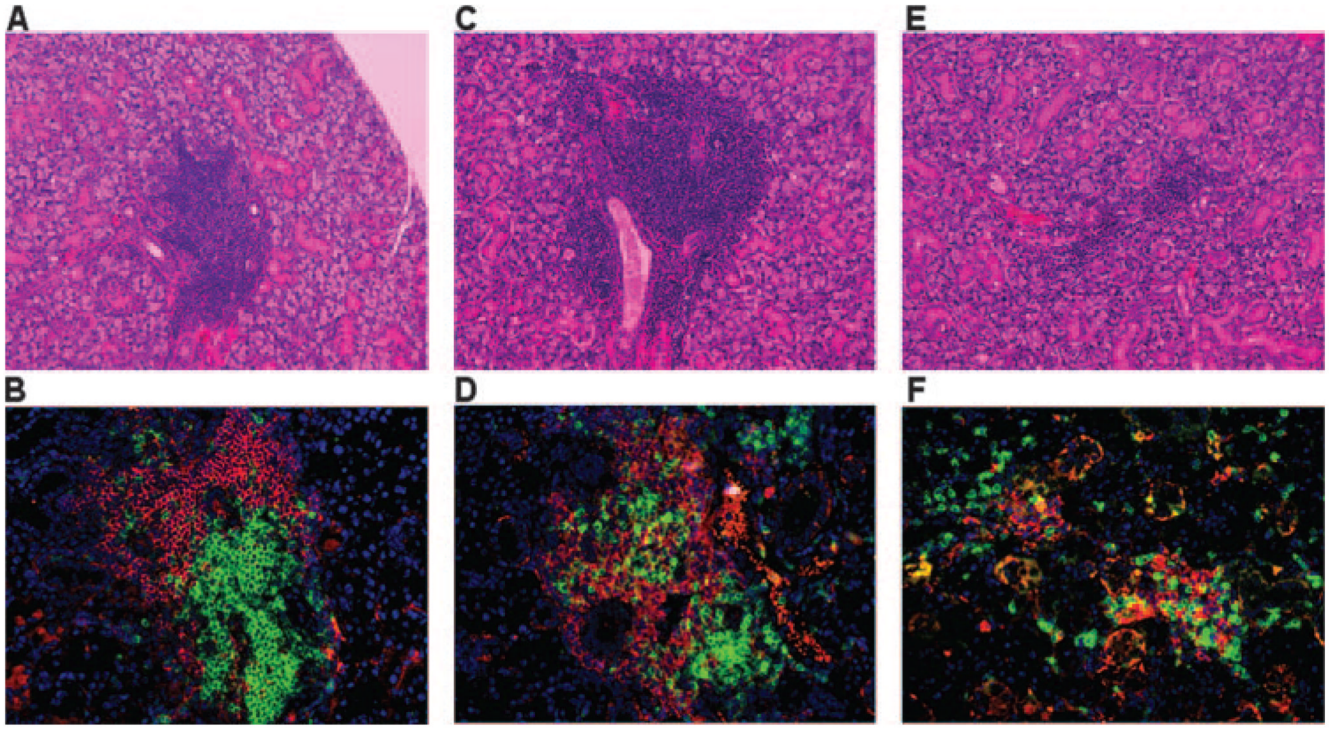

FIGURE 3.

Histological examination of the exocrine glands. Submandibular glands removed from groups of mice at ages ranging from 20 to 28 wk were fixed in 10% formalin. Each gland was serially sectioned (5-μm thickness) and histology performed on two sections cut 50 μm apart. Each section was stained with Mayer's H&E dye (*A*, *C*, and *E*) or immunofluorescent Abs for determining the distribution of B (anti-B220, red) and T (anti-CD3, green) cells in lymphocytic foci (*B*, *D*, and *F*). The sections were counterstained with 4′,6′-diamidino-2-phenylindole (DAPI) (blue). The numbers of focus were counted across whole histological sections of glands from 20-wk-old female NOD.B10-$H2^b$ mice (n = 8; *A* and *B*), 28-wk-old female NOD.B10-$H2^b$.C-$Stat6^{+/+}$ mice (n = 18; *C* and *D*), and 25-wk-old female NOD.B10-$H2^b$.C-$Stat6^{-/-}$ mice (n = 23; *E* and *F*). All H&E sections and immunofluorescent staining was examined at ×200 magnification. The number of foci for the two sections was averaged for comparisons.

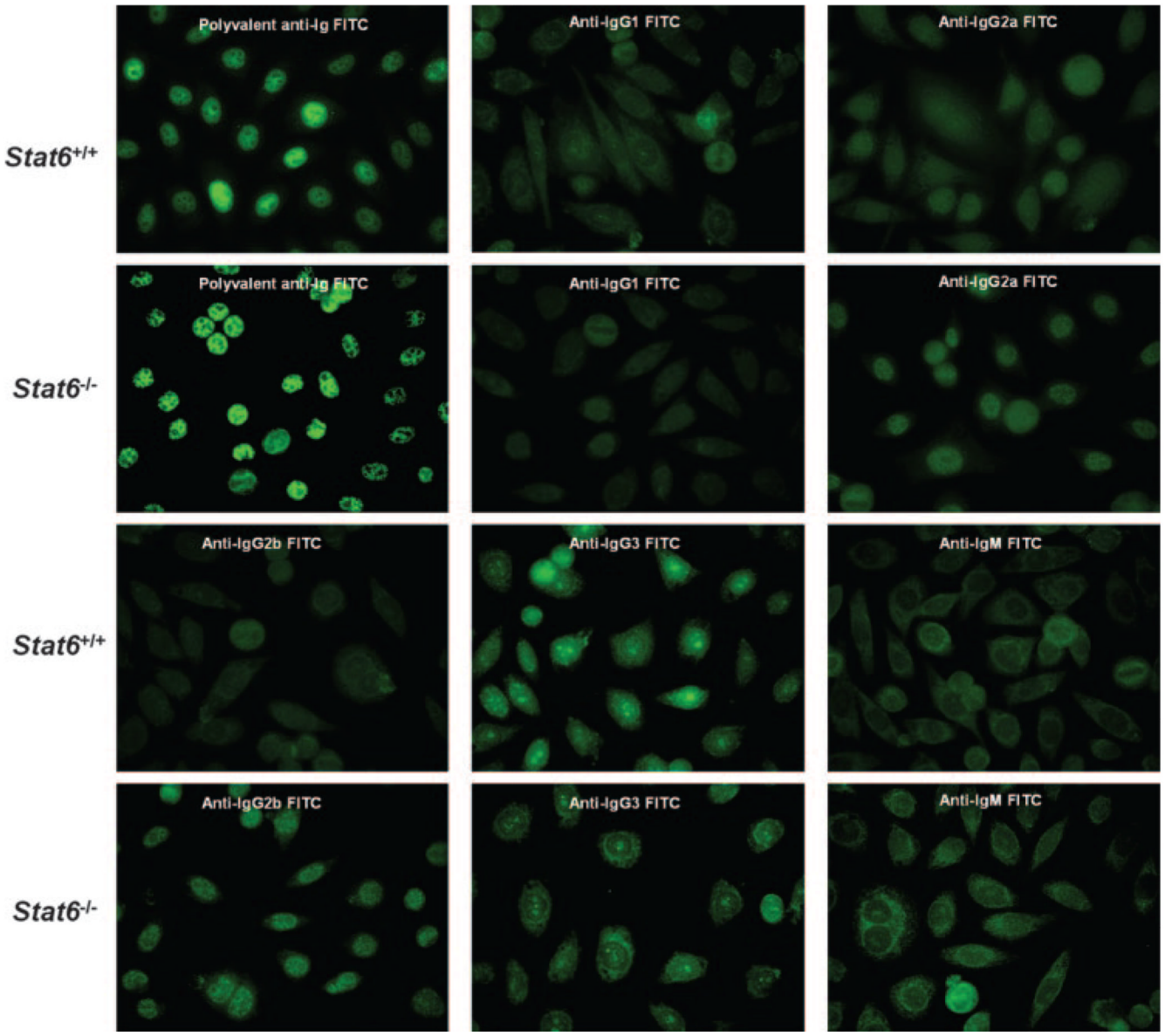

FIGURE 4.

Detection of ANAs. Serum samples obtained from groups of mice at various ages were pooled, diluted 1/40, and incubated with HEp-2-fixed substrate slides for 30 min at room temperature in a humidified chamber. The substrate slides were then incubated 30 min at room temperature with different isotype-specific secondary FITC-conjugated goat anti-mouse Abs diluted 1/50, then viewed using a Zeiss Axiovert 200 M fluorescent microscope at ×200 magnification. Sera—pooled from two mice selected from each experimental group of NOD.B10-*H2*^{b}.C-*Stat6*$^{+/+}$ and NOD.B10-*H2*^{b}.C-*Stat6*$^{-/-}$ mice—were used, and the experiment was repeated two additional times.

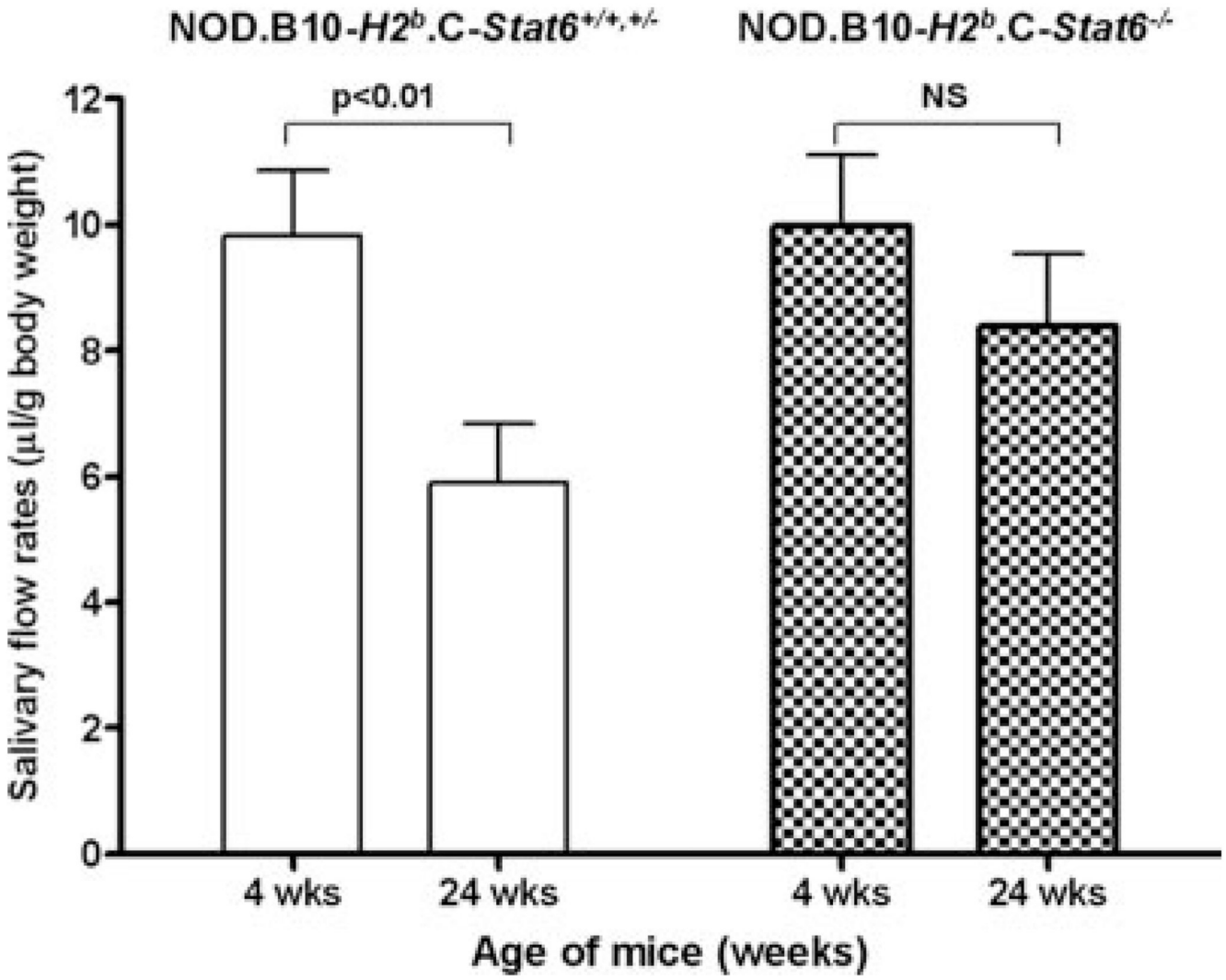

FIGURE 5.

Examination of stimulated salivary flow rates. Groups of 4-wk-old (n = 7) or 24-wk-old (n = 12) female NOD.B10-*H2*^{b}.C-*Stat6*$^{+/+}$ and NOD.B10-*H2*^{b}.C-*Stat6*$^{+/-}$ mice, and 4-wk-old (n = 5) or 24-wk-old (n = 8) NOD.B10-*H2*^{b}.C-*Stat6*$^{-/-}$ mice were injected with isoproterenol/pilocarpine to stimulate saliva secretion. Saliva was collected from each mouse for 10 min starting 1 min after injection of the secretagogue. The volume of each sample was measured. Statistical analysis was performed by Student Newman-Keuls test using GraphPad InStat software.

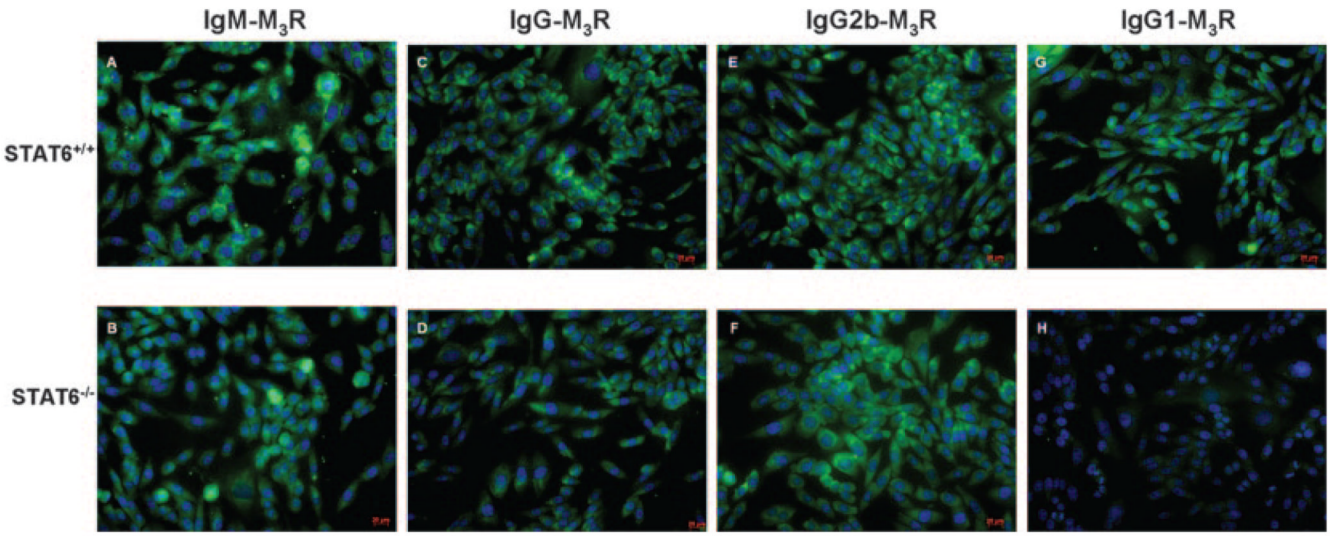

FIGURE 6.

Detection of M3R isotypic autoantibodies by immunofluorescence. Sera collected from NOD.B10-*H2*^{b}.C-*Stat6*$^{+/+}$ and NOD.B10-*H2*^{b}.C-*Stat6*$^{-/-}$ mice were incubated at a dilution of 1/50 with newly cloned M3R-transfected Flp-In CHO cells (see Ref. 14 and Ref. 19) for 1 h in a humidified chamber at room temperature. The cells were washed five times (5 min each wash) with PBS, then incubated 30 min at room temperature with FITC-conjugated secondary Abs specific for IgM (*A* and *B*), IgG (*C* and *D*), IgG2b (*E* and *F*), or IgG1 (*G* and *H*) isotypes diluted 1/100 (Serotec). Cells were again washed and visualized using a Zeiss Axiovert 200 M microscope at ×100 magnification. Images represent an exposure time of 25 ms.

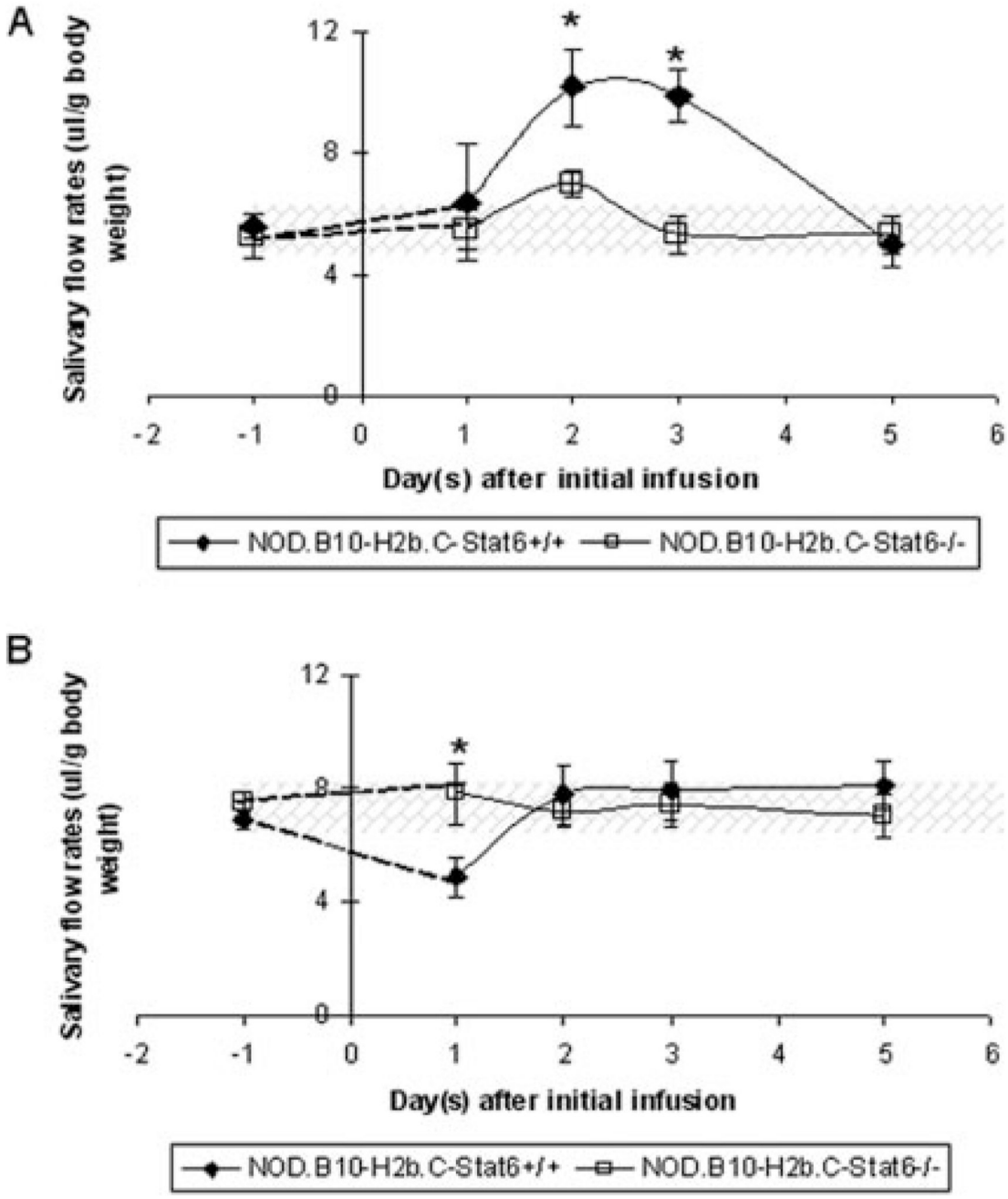

FIGURE 7.

Salivary flow rates of C57BL/6 mice after injections of IgG isolated from NOD.B10-*H2*^{b}.C-*Stat6*$^{+/+}$ or NOD.B10-*H2*^{b}.C-*Stat6*$^{-/-}$ mice. Temporal changes in salivary flow rates of male C57BL/6 mice injected with whole IgG collected from individual 6-wk-old NOD.B10-*H2*^{b}.C-*Stat6*$^{+/+}$(*n* = 4F) or NOD.B10-*H2*^{b}.C-*Stat6*$^{-/-}$ (*n* = 5M and 3F) mice (*A*) and 16-wk-old NOD.B10-*H2*^{b}.C-*Stat6*$^{+/+}$(*n* = 5F) and NOD.B10-*H2*^{b}.C-*Stat6*$^{-/-}$ (*n* = 2M and 3F) mice (*B*). Mice were injected i.p. with 500 μg of fractionated IgG. All values are expressed as mean salivary flow rates ± SEM. Statistical analysis was performed by two-tailed, paired Student *t* test using GraphPad InStat software (*, $p < 0.05$).

Table I

Levels of serum Ig isotypic Abs in NOD.B10-*H2*^{b}.C-*Stat6*$^{+/+}$ vs NOD.B10-*H2*^{b}.C-*Stat6*$^{-/-}$ mice

Ig Isotypes	C57BL/6J (*n* = 3)	NOD. B10-*H2*^{b} C-*Stat6*$^{+/+}$ (*n* = 5)	NOD. B10-*H2*^{b} C-*Stat6*$^{-/-}$ (*n* = 5)
IgM	91.6 ± 4.4[a]	112.7 ± 1.8	49.5 ± 1.9[b]
IgG1	345.7 ± 5.4	561.7 ± 4.6	60.5 ± 4.6[b]
IgG2a	150.6 ± 2.8	244.8 ± 6.7	149.4 ± 4.9[c]
IgG2b	38.5 ± 2.6	125.2 ± 1.3	100.2 ± 1.5[c]
IgG3	58.1 ± 3.0	58.0 ± 1.1	50.8 ± 1.1[b]
IgA	115.8 ± 1.1	115.8 ± 1.1	67.6 ± 1.3[b]
IgE	20.9 ± 1.4	60.8 ± 1.3	6.1 ± 0.9[b]

[a] Values are given as micrograms per milliliter ± SE.

[b] Value of $p < 0.001$ for comparisons between NOD.B10-*H2*^{b}.C-*Stat6*$^{+/+}$ and NOD.B10-*H2*^{b}.C-*Stat6*$^{-/-}$ mice.

[c] NS for comparisons between NOD. B10-*H2*^{b}.C-*Stat6*$^{+/+}$ and NOD.B10-*H2*^{b}.C-*Stat6*$^{-/-}$ mice.